npj | climate and atmospheric science

Article

Published in partnership with CECCR at King Abdulaziz University

https://doi.org/10.1038/s41612-025-00980-7

Testing GWP* to quantify non-CO_2 contributions in the carbon budget framework in overshoot scenarios

Matteo Mastropierro[1,2] ✉, Katsumasa Tanaka[2,3] ✉, Irina Melnikova[2,3] & Philippe Ciais[2]

The Global Warming Potential-star (GWP*) approach is a way to convert the emissions of short-lived climate forcers to CO_2-equivalent emissions while maintaining consistency with temperature outcomes. Here we evaluate the performance of GWP* when it is used to account for non-CO_2 gases within the carbon budget framework. We convert methane (CH_4) emissions to CO_2-equivalent emissions via GWP* and calculate the temperature through simple climate models. We show that GWP* can accurately convert CH_4 emissions to reproduce the temperature until 2100 under a variety of scenarios, including overshoot scenarios, except those with a rapid decline in CH_4 emissions. Beyond 2100, however, the use of GWP* can lead to temperature overestimation since it extends beyond its calibration range. Furthermore, we find that under scenarios designed to achieve identical temperature targets but with varying overshoot profiles, cumulative CO_2-eq budgets (GWP*-basis) generally increase with overshoot length and magnitude. This is driven by the internal dynamics of our model, as characterized by its negative zero-emission commitment. While the use of GWP* enhances such effects with increasing overshoot length, it exerts opposite effects with increasing overshoot magnitude.

Anthropogenic climate change is caused by emissions of a range of greenhouse gases (GHGs) that widely vary with respect to their radiative efficiency, atmospheric lifetime, and therefore impact on climate system[1]. To deal with GHGs of different characteristics on a common scale, the impact of non-CO_2 GHG emissions on climate is sometimes expressed in terms of CO_2 equivalent (CO_2-eq) emissions. In doing so, the emissions of non-CO_2 GHGs are converted to CO_2-eq emissions using GHG emission metrics[2]. The most widely used metric is the 100-year GWP (GWP100), which is defined as the time-integrated radiative forcing *over* 100 years following a pulse emission of one ton of a GHG divided by the corresponding quantity of one ton of CO_2[3,4]. Similarly, other metrics often considered are the GWP20 (with a 20-year reference time period) and the 100-year Global Temperature change Potential (GTP100), which is defined as the global temperature change following a pulse emission of one ton of a GHG *after* the reference time period of 100 years divided by the corresponding quantity of one ton of CO_2[5].

International climate treaties, such as the Kyoto Protocol and the Paris Agreement, commonly address multiple GHGs with the use of GWP100 to mitigate climate change cost-effectively[6–10]. However, when GWP100 is used to aggregate GHG emissions on a common scale of CO_2, the temperature impacts of different GHGs are not accurately captured owing to their diverse behavior in the atmosphere. GHGs fall into two categories: short-lived climate pollutants (SLCPs) and long-lived climate pollutants (LLCPs)[11]. There have been decades-long efforts to provide a more accurate emission metric in terms of the consistency with radiative forcing or temperature[5,12–16]. GWP100 is not a metric that intends to capture the contrasting temperature responses of LLCP and SLCP emissions[2,11,17,18].

CO_2, an LLCP, once emitted, will largely remain in the atmosphere (the so-called airborne fraction) with slightly declining concentrations for centuries to millennia[19–21]. The slightly declining concentrations lead to near-stable warming due to the thermal inertia of the ocean[22]. It is thus possible to relate cumulative CO_2 emissions to the temperature rise in an almost linear fashion through the widely used transient climate response to cumulative emissions (TCRE)[23,24]. This provides the basis for the 'remaining carbon budget approach', which is usually used for CO_2.

In contrast, CH_4, an SLCP, is mainly removed from the atmosphere due to atmospheric chemistry processes on faster time scales and thus has a smaller turnover time in this reservoir. It is currently an active research

[1]Department of Environmental Sciences, Statistics and informatics, Ca' Foscari University of Venice, Venice, Italy. [2]Laboratoire des Sciences du Climat et de l'Environnement (LSCE), IPSL, CEA/CNRS/UVSQ, Université Paris-Saclay, Gif-sur-Yvette, France. [3]Earth System Division, National Institute for Environmental Studies (NIES), Tsukuba, Japan. ✉e-mail: matteo.mastropierro@unive.it; katsumasa.tanaka@lsce.ipsl.fr

question how to determine the contribution of CH_4 and other SLCPs in the "carbon budget" framework[25–29]. Unlike CO_2, a pulse emission of CH_4 or other SLCPs does not result in near-stable warming; a stable warming is the consequence of a sustained or no increase in the rate of CH_4 emissions (or other SLCP emissions). In other words, a one-off emission of CO_2 is approximately comparable to a sustained increase in the emission rate of CH_4 in terms of the temperature outcome[30,31].

A new metric, GWP*, that captures this fundamental relationship has been proposed, allowing an integration of SLCPs into the carbon budget framework[16]. Starting from the work of Allen et al.[15], the GWP* metric was built by considering a 20-year time interval to assess the rate of changes in SLCP emissions. Cain et al.[16] further improved GWP* by incorporating the small multi-centennial warming effect arising from SLCP emissions, with an additional term representing the "stock" effect (comparable to the behavior of CO_2) on top of the term for the "flow" effect originally proposed. Therefore, GWP* can be defined by combining the effects from the emission itself (stock) and the change in emissions (flow), with the coefficients s and r, respectively, in Eq. (1). CO_2-eq emissions (E_{CO_2e}), which are referred to as CO_2-warming equivalent emissions when based on GWP* in Cain et al.[16], of SLCP emissions can be calculated as follows:

$$E_{CO2e} = GWP_H \times \left[r \times \frac{\triangle E_{\mathrm{SLCP}}}{\triangle t} \times H + s \times E_{SLCP} \right] \quad (1)$$

Here, the term ΔE_{SLCP} represents the change in the rate of SLCP emissions with respect to the preceding time interval Δt, whereas E_{SLCP} is the emission of the SLCP for that year, and GWP_H is the GWP value of the SLCP over the time horizon H. Originally, by fixing the coefficients r and s to 0.75 and 0.25, respectively, it was possible to ensure a good approximation of CH_4 impacts on temperatures over a range of emissions scenarios (RCP2.6, RCP4.5, and RCP6.0) until 2100[16,28]. Subsequently, a further modification was put forward to scale the right-hand side of Eq. (1) to ensure the forcing equivalency[32]. Finally, the GWP* equation adopted in the Sixth Assessment Report of the Intergovernmental Panel on Climate Change (IPCC AR6)[33,34], which is used in our analysis, is the following form:

$$E_{CO2e}(t) = 0.28 \times E_{100}(t) + 4.25 \times \left(E_{100}(t) - E_{100}(t-20) \right) \quad (2)$$

$E_{100}(t)$ denotes the emissions of an SLCP multiplied with its GWP100 value. The first and second terms on the right-hand side of Eq. (2) capture the stock and flow effects, respectively, with a much higher weight given on the flow effects. Equation (2) is a special case of Eq. (1) with the time interval $\triangle t$ of 20 years (also modified with a scaling factor of 1.13 discussed above). Note that this formula is based on GWP100 values in Table 8.A.1 of the IPCC AR5.

Although GWP* is often referred to as a metric, GWP* is not a single value: it is rather a more elaborated way of applying existing GWP100 values. In the traditional approach of using GWP100, the value of GWP100 for the non-CO_2 GHG of interest (for both SLCPs and LLCPs) is simply multiplied with the non-CO_2 GHG emissions to calculate CO_2-eq emissions. In the GWP* approach, however, the value of GWP100 is multiplied with the emissions and the change in the rate of emissions for a non-CO_2 GHG (for SLCPs only) as in Eq. (1). This approach allows for a more accurate translation of the temperature response of SLCP emissions to that of CO_2 emissions when calculating CO_2-eq emissions.

Scenarios that exceed the 1.5 °C or 2 °C warming target level temporarily (so-called overshoot scenarios), in which temperatures rise and then fall, are becoming increasingly relevant in the face of inadequate emission reduction commitments in the policy arena. Although GWP* was proposed with the aim of obtaining a more accurate estimate of temperature changes from cumulative CO_2-eq emissions, the performance of GWP* with declining emissions in overshoot scenarios was not fully assessed in IPCC AR6[35] and, at the moment of writing this manuscript, has yet to be systematically tested in any peer-reviewed papers.

Previous studies have relied either on specifying the non-CO_2 warming response for a given scenario and determining the CO_2 contribution as a residual[27,36] or on assuming and exploiting a scenario-dependent relationship between cumulative CO_2 emissions and non-CO_2 climate forcers[37]. Another recent approach relies on the concept of CO_2 forcing equivalent (CO_2-fe) emissions to consider the contributions of non-CO_2 climate forcers[29,38]. However, implications of using GWP* to determine non-CO_2 contributions to the carbon budget for overshoot scenarios have not been systematically explored.

This is particularly relevant to pathways achieving the 1.5 °C warming target, as around 90% of the scenarios considered in the IPCC Special Report on 1.5 °C (SR15) are either overshoot scenarios for the 1.5 °C target or, more generally, peak and decline scenarios[39]. Similarly, a large majority of low emissions scenarios developed from Integrated Assessment Models have been peak and decline scenarios[22], with more recently developed stabilization scenarios with net-zero CO_2 emissions being an exception[40,41]. Lastly, given the current emission trajectory and the recent anomalous warming, overshooting the 1.5 °C target level is projected to be imminent[42,43].

Moreover, there is a growing interest in the Earth system modeling community to simulate very long-term overshoot scenarios over a few to several centuries (up to 2300); such very long-term overshoot scenarios are under development in two Horizon Europe projects, RESCUE and OptimESM. GWP* could be considered as a convenient tool to assess the temperature implication of CH_4 emissions of such scenarios. Whereas GWP* may not be originally intended for such use, considering its calibration range to 2100, users of GWP* are not necessarily aware of the limitations associated with the calibration range clearly. It is therefore useful to assess how well GWP* serves its purpose over multi-century time scales with different lengths and magnitudes of overshoot.

Therefore, in this paper, we aim to tackle the following scientific questions: Does the GWP* metric adequately ensure equivalent temperature responses when it is used to convert SLCP emissions to CO_2-eq emissions under multi-century scenarios with different lengths and magnitudes of temperature overshoot? Can this metric be used to include non-CO_2 contributions in the carbon budget approach for overshoot scenarios?

Results

Testing the temperature equivalency of GWP* under SSPs

We first used a simple Impulse Response Function (IRF) model in IPCC AR5[1] to simulate the temperature effect of CH_4 emissions under the SSP1-1.9, SSP1-2.6, SSP4-3.4, SSP4-6.0, SSP5-3.4-OS, and SSP5-8.5 scenarios, up to the year 2300. We also calculated the temperature effect of the CO_2-eq emissions that were converted from the CH_4 emissions using different emission metrics, such as GWP100 and GWP*. By comparing the two results, we assessed the extent to which the temperature pathways are maintained or altered with the use of emission metrics in temperature calculations under different SSPs (i.e., "temperature equivalency").

Our results in Fig. 1 show that GWP100 ensures an imperfect but reasonably good temperature equivalency approximately up to the point of peak CH_4 emissions; however, its accuracy decreases substantially when CH_4 emissions decline, a well-known issue with GWP100. It is also shown that GWP100 performs better than GWP20 and GTP100 in terms of the temperature equivalency. GWP20 and GTP100 are illustrative of emphasizing and de-emphasizing, respectively, the temperature effect of CH_4 emissions relative to GWP100[44–46]. Thus, the results from GWP20 and GTP100 are opposite each other, relative to those from GWP100.

We further found that GWP* gives a nearly perfect temperature equivalency approximately until the end of the century under the range of emission scenarios. This result is rather expected, as GWP* is calibrated to do so under the three RCP scenarios. A notable exception is, however, that when CH_4 emissions drop sharply, GWP* overestimates the cooling effect, as shown most evidently under SSP5-3.4-OS (Fig. 1e). This behavior reflects the fact that none of the RCP scenarios used to calibrate GWP* contain a large overshoot as in SSP5-3.4-OS. It should also be emphasized that, compared to GWP100, GWP* clearly shows superior performances for

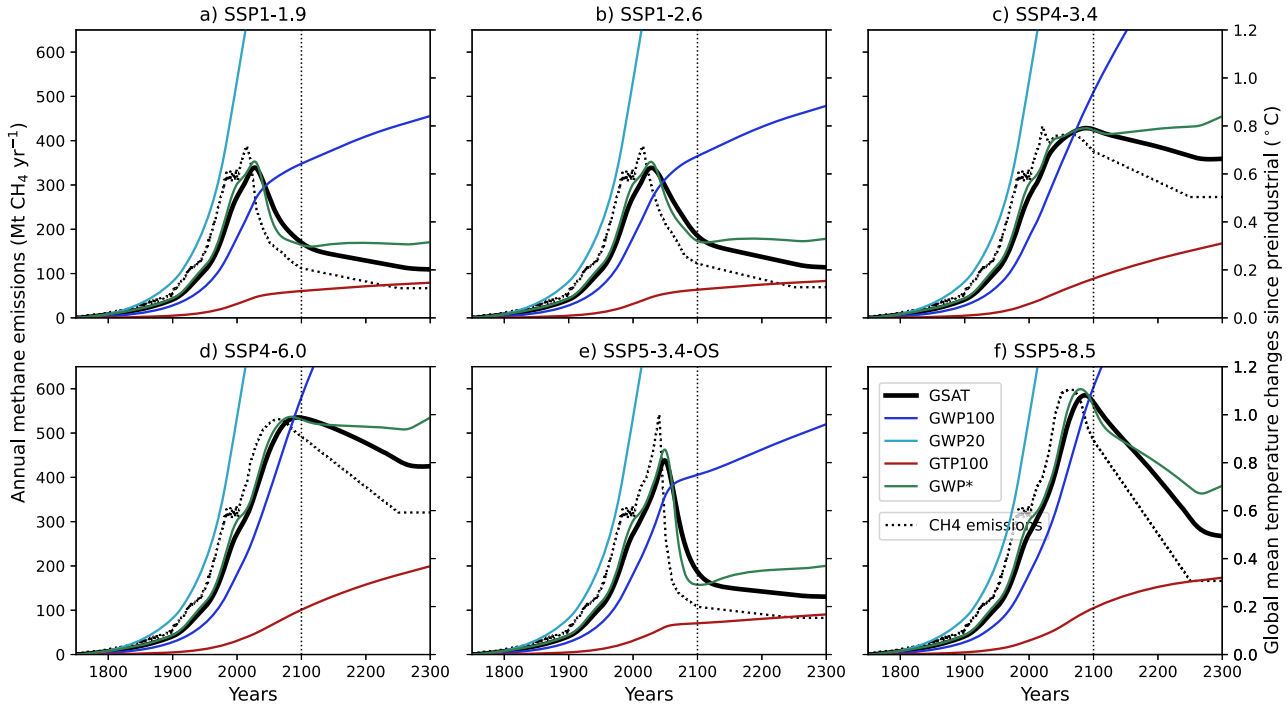

Fig. 1 | Temperature responses to CO_2-eq emissions computed from CH_4 emissions in SSP scenarios using different emission metrics. a–f represents different SSP scenarios. Dotted black lines indicate CH_4 emissions of each SSP. Thick black lines give the temperature response calculated with the IRF for CH4 emissions without using any emission metric. Thin solid lines show the temperature response calculated with the IRF for CO_2-eq emissions converted from the CH_4 emissions using different metrics such as GWP100 and GWP*. Only the CH_4 emissions or the CO_2-eq emissions converted from CH_4 emissions are considered for temperature calculations here. The temperature calculation is based on the IRF. This figure mimics but extends the presentation of Figure 7.22 of IPCC AR6 WGI, which shows the outcome only till 2100.

reproducing the temperature (Table S1). Over the longer run, however, the temperature equivalency provided by GWP* no longer holds. The cooling effect of CH_4 is underestimated or shown even as a slight warming with the use of this metric when CH_4 emissions decrease (in all SSPs). From the physical perspective, this is due to the fact that the "stock" parameter, as defined in Cain et al., (2019), emphasize too much the century-timescale response to earlier methane emission increases, leading to an overestimation of temperatures beyond 2100. These findings are robust since the deviations discussed here are generally confirmed by two other modeling approaches (Fig. S1). Our findings raise the question regarding whether the use of GWP* could be adequate for accounting for the contribution of CH_4 emissions in the carbon budget framework when it is applied for overshoot scenarios, in particular beyond 2100.

We then explored the sensitivity of the foregoing results to the parameters used to define GWP*. We first investigated the sensitivity with respect to the time interval considered between two pulse emissions in the flow term of Eq. 2 (20 years by default, Fig. S2a). By minimizing the Sum of Squared Errors (SSE) between the temperatures calculated from original CH_4 emissions and that from CO_2-eq emissions based on the modified GWP* for all the scenarios in the period 1750-2100, we found the optimal time interval to be 22 years, which is close to the commonly used value of 20 years. Furthermore, we investigated the sensitivity with respect to the formulation of the flow term in the GWP* equation by substituting the default flow term taking the change in emissions 20 years apart (Eq. 2) with an alternative flow term taking the *average* change in emissions over the previous 5, 10, 20, 30, 40 or 50 years (Fig. S2b). Our results show that the use of average change in emissions over the previous 40 years or longer leads to the best temperature equivalency. We further found that the use of average change in emissions over the previous 40 years yielded a slightly better temperature equivalency than the use of emissions 20 years apart. We can explain this outcome by the fact that the use of average emissions over 40 years, compared to the use of two end-point emissions 20 years apart, more closely resembles the exact CO_2-eq emissions that precisely reproduce the warming from original CH_4 emissions (i.e., the Linear Warming Equivalence emissions)[47]. However, even when the GWP* equation is modified in several different ways, the temperature misfit after the rapid drop in CH_4 emissions persists (Fig. S3).

Using GWP* to quantify the overshoot CO_2-eq budget

Our analysis based on the SSP scenarios has shown that the temperature equivalency of GWP* can be influenced by the rate of CH_4 emission reductions. To gain more insights, we performed a further analysis based on scenarios with different overshoot lengths and magnitudes. To generate a range of overshoot scenarios, we used the Aggregated Carbon Cycle, Atmospheric Chemistry, and Climate (ACC2) model[9,22,48]. ACC2 is a simple climate model[49] that resolves many GHGs and aerosols, accounting for primarily important nonlinearities in the global earth system such as CO_2 fertilization of the land biosphere, saturation of ocean CO_2 uptake under rising atmospheric CO_2 concentrations, and climate-carbon cycle feedback. The interaction between CH_4 and tropospheric ozone through the OH chemistry is parameterized in ACC2. The temperature is calculated by using a land-ocean energy balance model coupled with a heat diffusion model (see "Methods" for details). The simple climate model ACC2 can be further coupled with a climate mitigation module consisting of a set of marginal abatement cost functions[9,50] to calculate least-cost emission pathways for a specified climate target. ACC2 then works as an optimizing climate-economy model, and we took advantage of this model feature to systematically generate overshoot pathways for our analysis. We also took advantage of the more detailed process representations of ACC2, relative to the IRF model, while simplicity is maintained in ACC2 for performing sensitivity simulations.

We use ACC2 to generate a range of pathways that reach the 1.5 or 2 °C target level after overshoot of varying lengths and magnitudes. We calculate least-cost emission scenarios to keep the temperature below a target level throughout the simulation period (temperature *stabilization* pathways). If

we apply the temperature target only after a certain year, the model yields least-cost emission scenarios that lead to temperature *overshoot* pathways. In this case, the temperature exceeds the target level before that year, since it is less costly to invest in mitigation efforts later in the cost-effectiveness framework as also pointed out by previous studies[51,52]. The length and the magnitude of the temperature overshoot are determined by ACC2's internal cost minimization reflecting assumptions on the maximum rates of emission abatements and the discounting rate. We varied the target years between 2060 and 2180 with an interval of 10 years and selected appropriate target years to be tested for each temperature goal (1.5 °C and 2 °C). For each target year, we further varied the discount rate to 2% and 6%, compared to the original 4% by default, to generate different overshoot magnitudes, while keeping the same overshoot length. Emissions of all climate forcers other than CO_2 and CH_4 are assumed to follow SSP1-1.9 and SSP1-2.6 in the case of the 1.5 and 2 °C targets, respectively.

For each pathway, we calculated the "overshoot CO_2-eq budget" which is defined as the cumulative net CO_2-eq emissions (GtCeq) from 2020 till the year when the temperature stabilizes at or returns to the 1.5 or 2 °C warming target level after temperature overshoot. The overshoot CO_2-eq budget discussed in this paper implicitly assumes that positive and negative emissions can be equally balanced, although the validity of this assumption will be explored later in this paper. The carbon budget for this time frame is referred to as the threshold return budget elsewhere[25,53], but we include non-CO_2 contributions in the threshold return budget using the emission metric approach: GWP* for SLCPs and GWP100 for LLCPs. For the sake of analysis, our overshoot CO_2-eq budget considers only CO_2 and CH_4, unless stated otherwise, which are our focus but are largely representative of the entire CO_2-eq budget because these two gases are usually most important for climate change mitigation. We present the results calculated from ACC2 emulating IPSL-CM6A-LR in the main paper. Qualitatively similar results can be found from ACC2 emulating other ESMs, as in Figs. S4 and S5 for CNRM-ESM2-1 and MIROC-ES2L.

Multi-gas optimization experiments. We first performed *multi-gas* optimization experiments (Fig. 2), where CO_2 and CH_4 emission pathways are optimized simultaneously using the ACC2 setup to calculate the least-cost pathways, while all other gases and pollutants are assumed to follow SSP1-1.9 and SSP1-2.6 in the case of the 1.5 °C (Fig. 2a, c) and 2 °C target (Fig. 2b, d), respectively. Panels (a) and (b) of Fig. 2 show the overshoot CO_2-eq budget (with CH_4 converted via GWP*) for different 1.5 °C and 2 °C stabilization years, respectively, with ranges of overshoot magnitude and length. For both the 1.5 °C and 2 °C target year simulations, we found that the longer the temperature overshoot is, the larger the overshoot CO_2-eq budget is. Furthermore, for the same overshoot length, the higher the overshoot is, the larger the overshoot CO_2-eq budget is (the 2 °C case with the 2060 target year is an exception because

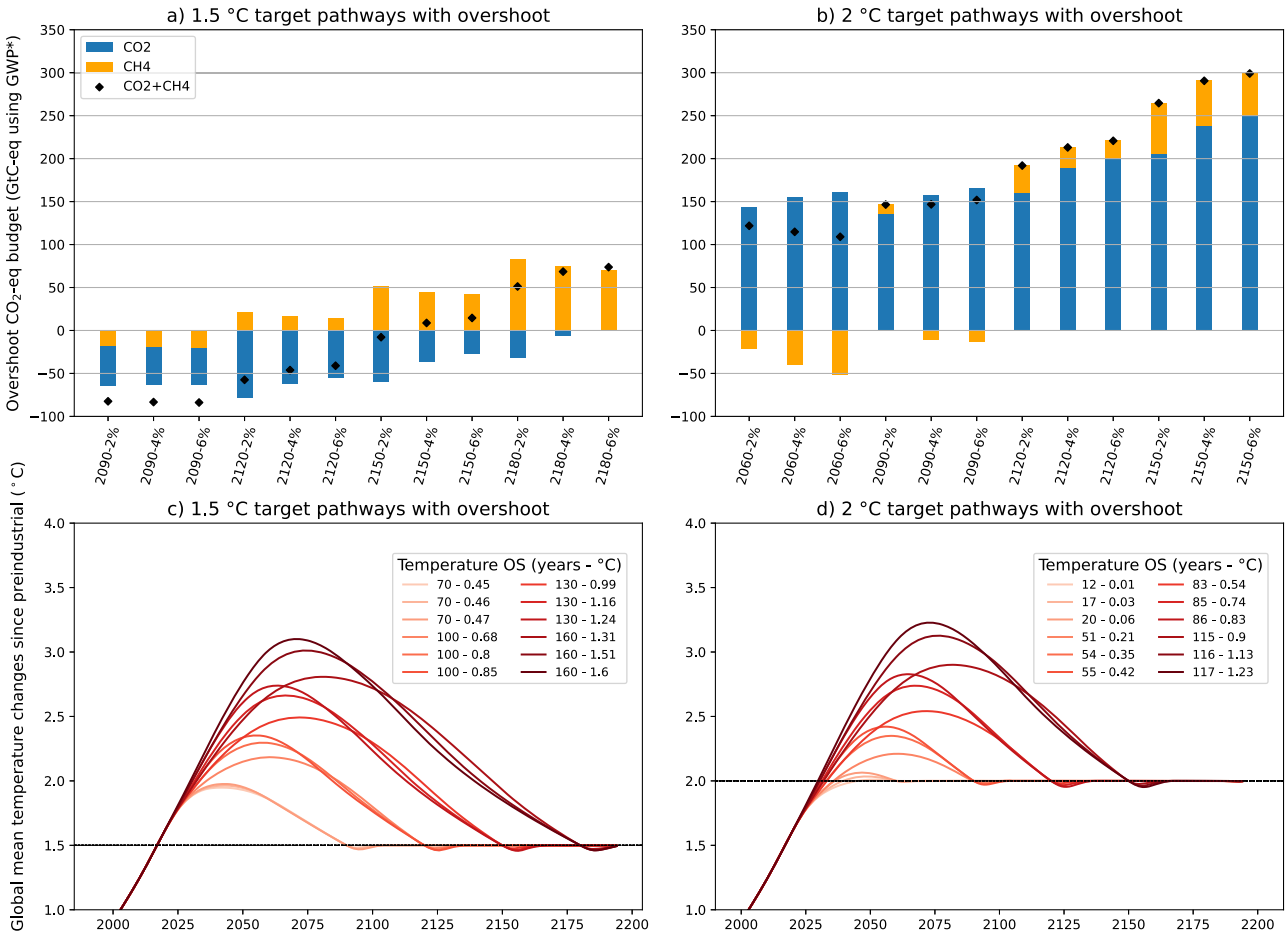

Fig. 2 | Overshoot CO_2-eq budgets of least-cost pathways for the 1.5 and 2 °C target levels with temperature overshoot of varying lengths and magnitudes (multi-gas optimization experiment). a, **c** shows the overshoot CO_2-eq budget and temperature pathways for the 1.5 °C scenarios, whereas (**b**, **d**) shows those of the 2 °C scenarios. Both CO_2 and CH_4 emission pathways were optimized using ACC2 (emulating IPSL-CM6A-LR) for each target level and year with different discounting, with all other gases and pollutants following respective SSPs (SSP1-1.9 and SSP1-2.6 for the 1.5 and 2 °C target level, respectively). The figure shows the results of a combination of four different overshoot lengths and three different overshoot magnitudes for each temperature target level. The overshoot CO_2-eq budgets presented in this figure account for contributions from CO_2 and CH_4. The contributions of CH_4 in the overshoot CO_2-eq budget are determined using GWP*. Legends in panels c) and d) represent the duration (years) and magnitude (°C) of temperature overshoot relative to the 1.5 °C or 2 °C target level, respectively.

Table 1 | The effect of different overshoot profiles on the CO_2-eq budget under multi-gas, CO_2-only, and CH_4-only optimization scenarios for the 1.5 and 2 °C targets

	Multi-gas optimization scenarios	CO_2-only optimization scenarios	CH_4-only optimization scenarios
Increasing overshoot length	Increase in CO_2-eq budget	Increase in CO_2-eq budget	Increase in CO_2-eq budget
Increasing overshoot magnitude	Increase in CO_2-eq budget	Increase in CO_2-eq budget	Decrease in CO_2-eq budget

This table summarizes how the overshoot length and magnitude can generally affect the overshoot CO_2-eq budget for scenarios aiming for identical long-term temperature targets (1.5 or 2 °C warming) as derived by ACC2. See text for further details and discussions

the target lengths and magnitudes are not clearly separated) (Table 1). The increasing total overshoot CO_2-eq budget with increasing overshoot lengths and magnitudes reflects both the model behavior of ACC2 and the conversion of CH_4 emissions to CO_2-eq emissions via GWP*, which will be disentangled in the analysis presented in the next section.

The contribution of CH_4 in the overshoot CO_2-eq budget becomes particularly important for 1.5 °C pathways, in which the total overshoot CO_2-eq budget is so small that the contribution from CH_4 can even determine the sign of the total overshoot CO_2-eq budget. This indicates that how to account for CH_4 contributions to the overshoot CO_2-eq budget is crucial for mitigation pathways aiming at the 1.5 °C target level. The overshoot CO_2-eq budgets calculated with our default version of ACC2 are generally low because this version of ACC2 was configured to IPSL-CM6A-LR, which exhibits a high climate sensitivity (Table S4 and Figs. S10 and S11). The overshoot CO_2-eq budget is in fact already negative in about a half of the cases for the 1.5 °C target level, specifically for scenarios with target years in 2090 and 2120. These negative overshoot CO_2-eq budgets reflect deep CO_2 mitigation that is required to compensate for the limited CH_4 mitigation (Fig. S6 for simulations for the target year of 2120 with three different overshoot profiles), as well as the unmasked warming from decreasing emissions of air pollutants (following SSP1-1.9 for 1.5 °C target scenarios). In the remaining cases with high and long overshoots, on the other hand, some more emissions are still left in the budget.

Single-gas optimization experiments. We further performed *single-gas* optimization experiments (Fig. 3). In this case, only the emission pathway of one of the two gases (CO_2 or CH_4) is optimized to reach the target temperature with lowest cost, while the emission pathways of all other gases and pollutants are kept at the respective SSP scenario (SSP1-1.9 or SSP1-2.6) corresponding to the target temperature (1.5 or 2 °C target level). This experiment is useful to isolate the relative contribution of CO_2 and CH_4 to the overshoot CO_2-eq budget. That is, unlike the previous experiments, in which emission reductions of CO_2 and CH_4 can be traded to yield a least-cost solution, emission reductions of only one gas can change with varying overshoot lengths and magnitudes in these experiments.

As for Fig. 2, panels a) and b) of Fig. 3 report the overshoot CO_2-eq budget calculated for each simulation of the single-gas optimization experiments, for CO_2 cumulative emissions and CO_2-eq cumulative emissions (CH_4 converted with GWP*), respectively. In the case of CO_2-only optimization experiment (Fig. 3a), the longer the temperature overshoot is, the larger the overshoot CO_2-eq budget is. This finding is in contrast to the general belief that the carbon budget is reduced with increasing overshoot lengths[54,55]. We found qualitatively similar results for the CH_4-only optimization experiment as well (Fig. 3b). Caution must be taken in drawing conclusions from this, as it could be interpreted that a late mitigation is preferred compared to early mitigation actions. It should be noted that this finding is dependent on model assumptions, such as CO_2 fertilization effect (Figure S8), and model characteristics as discussed in the next section.

The results for overshoot magnitudes provide a further insight: the higher the overshoot is for the same overshoot length, the larger the overshoot CO_2-eq budget is from the CO_2-only optimization experiment, but the smaller the overshoot CO_2-eq budget is from the CH_4-only optimization experiment (in most cases). The results of the CO_2-only optimization experiment reflect the dynamic behavior of ACC2 (analyzed in the next section); those of the CH_4-only optimization experiment, on the other hand, not only reflect the model's dynamic behavior but also the conversion of CH_4 emissions to CO_2-eq emissions via GWP*. In the analysis that follows, we further delve into this finding separately in the ramp-up and ramp-down periods of overshoot scenarios. Note that CH_4 contributions to the overshoot CO_2-eq budget of the CH_4-only optimization experiment are higher in the 1.5 °C target case than those in the 2 °C target case, which appears counterintuitive first since a lower temperature target usually implies stricter emission limits. This phenomenon is due to the higher relative contributions of the prescribed CO_2 baseline scenario to the total radiative forcing in SSP1-2.6 (used for the 2 °C target simulations) compared to those in SSP1-1.9 (used for the 1.5 °C target simulations).

TCRE of the ramp-up and ramp-down phases of overshoot scenarios

To gain insight into how the model's dynamic behavior influences the overshoot CO_2-eq budget in different phases of overshoot scenarios, we looked into the TCRE separately for the ramp-up and ramp-down phases. We computed TCRE, for each single-gas optimization experiment, as the ratio of the temperature change over the cumulative CO_2-eq emissions for the sum of three gases (CO_2, GWP*-weighted CH_4, and GWP100-weighted N_2O). We distinguish TCRE between the ramp-up (from year 1750 to the year of peak emissions) and the ramp-down phases (from the year of peak emissions to the year when the temperature target is met after overshoot) as TCRE+ and TCRE−, respectively. The current literature does not provide sufficient clarity regarding the extent to which the linear relationship between cumulative CO_2 emissions and temperature changes holds in case of negative emissions[56]. As reported in Chapter 5 of IPCC AR6 WGI, there is no clear agreement among models for the relationship between TCRE+ and TCRE−[35]. Figure 4 shows the results from both the CO_2-only optimization and CH_4-only optimization experiments for the 1.5 °C target. In Fig. 4a, c, cumulative emissions consider only one gas (CO_2 or GWP*-weighted CH_4), but the warming is calculated from the emissions of all gases, indicating that the cumulative emissions are not necessarily consistent with the simulated warming. In Fig. 4b, d, on the other hand, cumulative emissions consider the three major gases, which is thus approximately consistent with the simulated warming, but the effects from individual gases cannot be isolated. The values of TCRE+ and TCRE− (°C/1,000 GtCeq) reported in panels b) and d) represent the mean of all TCRE+ and TCRE− values from the scenarios presented in the panels. The general indication is that TCRE− is larger than TCRE+, which is consistent with the finding from Fig. 2 and Fig. 3: the longer or higher the temperature overshoot is, the larger the overshoot CO_2-eq budget is. An exception is the decreasing TCRE− with increasing overshoot magnitudes from the CH_4-only optimization experiments (Fig. 4d). By taking the average of TCRE− across the scenarios with low, medium, and high overshoot (i.e., for discount rates of 2%, 4%, and 6%), the TCRE− values are indeed decreasing with increasing overshoot magnitudes, which are 3.1, 2.9, and 2.7, respectively (mean value of 2.9, as reported in Fig. 4d). This can be confirmed with our earlier finding that the overshoot CO_2-eq budget decreases with increasing overshoot magnitudes in the CH_4-only optimization experiment owing to the use of GWP*.

The relatively large TCRE− from the CO_2-only optimization experiment can be further confirmed with the Zero Emission Commitment (ZEC) parameters of this model. Following the ZEC Model Intercomparison Project (ZECMIP) framework described in Jones et al.[57], we performed the

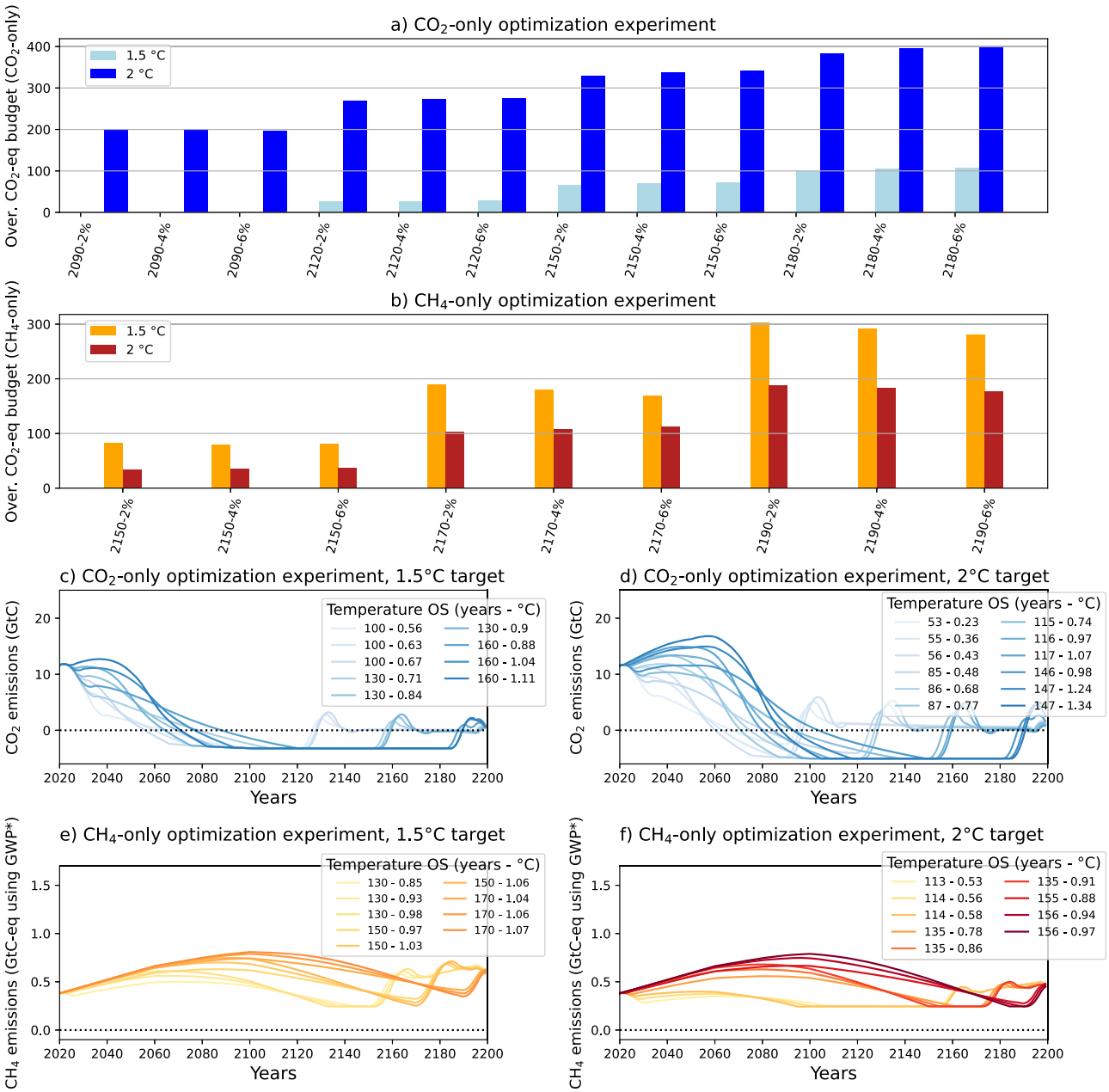

Fig. 3 | Overshoot CO_2-eq budgets of least-cost pathways for the 1.5 and 2 °C target levels with temperature overshoot of varying lengths and magnitudes (single-gas optimization experiment). **a**, **b** show the overshoot CO_2-eq budget for CO_2 and CH_4 optimization simulations, for different scenarios. The overshoot CO_2-eq budgets in panel a) represent only the contributions from CO_2. Those in (**b**) represent contributions from CH_4. **c**, **d** describe the emissions pathways for the 1.5 °C and 2 °C for CO_2 simulations. **e**, **f** describe the emissions pathways for the 1.5 °C and 2 °C for CH_4 simulations. Either CO_2 or CH_4 emission pathways were optimized using ACC2 (emulating IPSL-CM6A-LR) for each target level and year with different discounting, with all other gases and pollutants following respective SSPs (SSP1-1.9 and SSP1-2.6 for the 1.5 and 2 °C target level, respectively). The contributions of CH_4 in the overshoot CO_2-eq budget were determined using GWP*. Legends in (**c**–**f**) represent the duration (years) and magnitude (°C) of temperature overshoot relative to the 1.5 °C and or 2 °C target level, respectively.

B.1, B.2, and B.3 experiments as in MacDougall et al.[58] to compute the ZEC parameters (Fig. S9). These three experiments use 100-year bell-shaped CO_2 emissions of 1000 GtC, 750 GtC, and 2000 GtC, respectively, starting from pre-industrial conditions, aiming to assess the model-specific climate inertia in the decades after a complete cessation of emissions. We report the estimates of ZEC25, ZEC50, and ZEC90, representing the temperature change respectively 25, 50, and 90 years after the start of zero emissions. Table 2 shows that all three ZEC parameters are negative for ACC2, which supports the large TCRE− relative to TCRE+. We further note that the ZEC parameters for different configurations of ACC2 (emulated to CNRM-ESM2-1 and MIROC-ES2L used for sensitivity analyses) also present negative values (Fig. S9).

It should be emphasized that there is generally no consensus for the relationship between TCRE+ and TCRE−, among models, as demonstrated by previous studies[54,55,59–62]. The lack of consensus is also evident from the analysis of 1pct-CO_2-cdr idealized experiment[56], where MIROC-ES2L and CanESM5 report larger TCRE− than TCRE+ whereas UKESM1-0-LL and ACCESS-ESM1-5 show smaller TCRE+ than TCRE− (Fig. S12).

Discussion

This study examined how the emissions of non-CO_2 GHGs, in particular CH_4, can be accounted for in the overshoot CO_2-eq budget framework. A key requirement for including non-CO_2 contributions in the CO_2-eq budget framework is to ensure the temperature equivalency. That is, non-CO_2

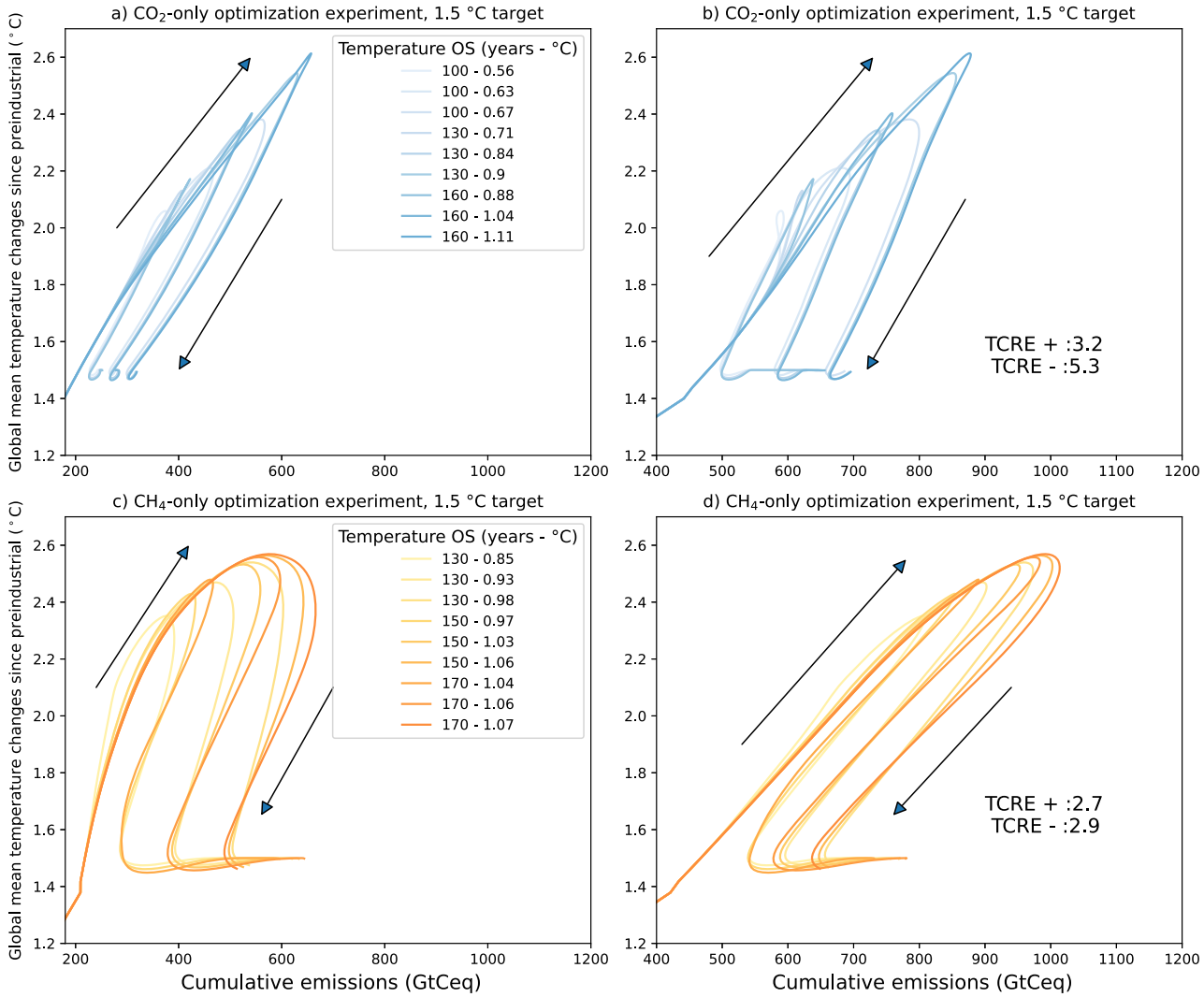

Fig. 4 | TCRE calculated from the single-gas optimization experiment for the 1.5 °C target using ACC2 emulating IPSL-CM6A-LR. a, **b** show the relationship between the temperature change and the cumulative emissions considering only CO_2 and the sum of CO_2, CH_4, and N_2O, respectively, for the period 2020-2200 from the CO_2-only optimization experiment. **c**, **d** show the relationship between the temperature change and the cumulative emissions considering only CH_4 and the sum of CO_2, CH_4, and N_2O, respectively, also for the same period but from the CH_4-only optimization experiment. CH_4 emissions were converted to CO_2-eq emissions with GWP*, whereas N_2O emissions were converted to CO_2-eq emissions with GWP100. Arrows indicate the direction of time.

emissions should be converted to CO_2-eq emissions in such a way that the implied temperature outcome remains the same. Recently, the GWP* approach has received attention; however, this approach has not been extensively evaluated for overshoot scenarios or, more generally, peak and decline scenarios in a long time scale.

Our analysis using the SSP scenarios confirmed that GWP* does a reasonably good job of ensuring a temperature equivalency for a range of pathways up to 2100 when it is used to convert CH_4 emissions to CO_2-eq emissions. An exception is that when the temperature drops sharply in the ramp-down phase of overshoot, the use of GWP* leads to an overestimation of cooling. Over a longer time scale up to 2300, when the temperature decreases moderately, the use of GWP* can lead to an underestimation of cooling or indicate a slight warming instead. These findings are related to the fact that GWP* was tuned to a certain set of pathways up to 2100. Our results indeed showed that the deviation tends to become more evident after 2100. These findings suggest that GWP* should be cautiously used for scenarios with strong decline in temperatures and/or longer-term peak and decline scenarios beyond 2100.

Nevertheless, GWP* is still far superior to the standard and most widely used metric GWP100 in terms of the temperature equivalency under all scenarios. We have attempted to improve GWP* by modifying the parameters in the GWP* equation, but this did not result in any substantial improvement in temperature equivalency.

It should be noted that the IRF was used for temperature calculations here in order to be consistent with the underlying methods used to derive metric values in AR5 and the GWP* formula in AR6. When ACC2 and FaIR are used for temperature calculations, our general findings still hold; however, the quantitative results become different particularly from ACC2, reiterating the fact that the GWP* formula is model-dependent or reflects certain model assumptions, a point that deserves more attention.

Our study further investigated how the overshoot CO_2-eq budget for the 1.5 and 2 °C target levels, including the contribution of CH_4 based on GWP*, can be affected by the temperature overshoot of varying lengths and magnitudes. We generated a set of scenarios to reach the representative temperature target levels with overshoot of different lengths and magnitudes through cost-effective calculations of ACC2 configured to several different state-of-the-art ESMs. Our results generally showed that the overshoot CO_2-eq budget increases with the length and magnitude of overshoot, except under CH_4-varying scenarios with different overshoot magnitudes. This finding is mainly related to the model property of ACC2 that it takes larger cumulative CO_2 emissions in absolute terms to produce a given amount of warming than it takes to produce the same amount of cooling in

Table 2 | ZEC values for ACC2 and other ESMs and EMICs participating at the ZECMIP framework[57]

Model	Model type	ZEC_{25} (°C)	ZEC_{50} (°C)	ZEC_{90} (°C)
ACC2 (emulating IPSL-CM6A-LR (default))	Simple climate model	−0.154	−0.282	−0.427
ACC2 (emulating CNRM-ESM2-1 (sensitivity))	Simple climate model	−0.168	−0.285	−0.403
ACC2 (emulating MIROC-ES2L (sensitivity))	Simple climate model	−0.136	−0.229	−0.322
Bern3D-LPX-ECS2K	EMIC	−0.057	−0.118	−0.158
DCESS1.0	EMIC	−0.050	−0.117	−0.212
GFDL-ESM2M	ESM	−0.154	−0.221	0.075
IAPRAS	EMIC	−0.060	−0.210	−0.420
LOVECLIM	EMIC	−0.002	0.102	0.001
MESM	ESM	−0.029	−0.113	−0.158
MIROC-lite-LCM	EMIC	−0.041	−0.056	−0.081
PLASIM-GENIE	EMIC	−0.151	−0.480	−0.684
UVicESCM2.10	EMIC	−0.034	−0.030	0.001
Mean		−0.0863	−0.170	−0.232

The table shows the results computed from data available at the ZECMIP data repository (http://terra.seos.uvic.ca/ZEC/) for the B.1 simulations described in Jones et al., (2019) and MacDougall et al., (2020)[57,58]. ACC2 emulating IPSL-CM6A-LR is used as default in our analysis, while those emulating CNRM-ESM2-1 and MIROC-ES2L are used for sensitivity analyses

absolute terms. In other words, TCRE+ is smaller than TCRE− in ACC2, which is also consistent with the negative ZEC, found in our analysis for ACC2. Importantly, this finding is modified by the conversion of CH_4 emissions into CO_2-eq emissions via GWP*. The application of GWP* on CH_4 has an effect of decreasing the apparent overshoot CO_2-eq budget with increasing overshoot magnitudes.

To summarize, the use of GWP* to include CH_4 in the CO_2-eq budget framework in case of overshoot scenarios works in most scenario until 2100, except for cases with a rapid decline in CH_4 emissions. Over a longer run beyond 2100, the use of GWP* can overestimate the warming effect of CH_4 emissions and consequently may lead to an overestimation of CO_2-eq budget. It should however be noted that these results depend on the model configuration used for the analysis, requiring further studies based on different modeling approaches, including uncertainty analyses of Earth system feedbacks.

Methods

Description of three reduced-complexity models

Our analysis used three different reduced-complexity models as follows in the order of increasing complexity: the Impulse Response Function (IRF) model of IPCC AR5[1], the Finite Amplitude Impulse Response (FaIR) model[63,64], and the Aggregated Carbon Cycle, Atmospheric Chemistry, and Climate (ACC2) Model[9,22,48].

First, the IRF model is a simplified representation of the atmospheric response to a pulse emission of CO_2. It approximates the fraction of emitted carbon that remains in the atmosphere over time[21], to estimate the temperature impact of GHG emissions according to the radiative efficiencies of the single GHG. The IRF model used in our study is derived from the latest estimates summarized in the IPCC AR5. It is employed to estimate the temperature response of CO_2-eq emissions derived from CH_4 using various conversion metrics.

Second, the FaIR v1.3 has been extensively used for assessing the temperature impacts of different emissions pathways and mitigation scenarios[16,27,38,65]. FaIR has a simple representation of the carbon cycle and accounts for nonlinear feedback such as the temperature and saturation dependency of land and ocean carbon sinks. The model calculates both CO_2 and non-CO_2 GHG atmospheric concentrations by tracking their time-integrated airborne fraction from their initial emissions. From concentrations, Effective Radiative Forcing (ERF) for thirteen forcings, including land-use change, tropospheric and stratospheric O_3 as well as other GHG are computed; finally the temperature change is calculated as the sum of its slow and fast components, representing temperature changes from a response to forcing from the upper ocean and the deep ocean, respectively.

Third, ACC2 is a simple climate-economy model composed of four modules: i) carbon cycle, ii) atmospheric chemistry, iii) physical climate, and iv) economy. The carbon cycle module is made of three ocean boxes, a coupled atmosphere-mixed layer box, and four land boxes. The physical climate module is the land-ocean energy balance model coupled with the heat diffusion model DOECLIM, which is used to calculate the temperature response to radiative forcing[48]. The radiative forcing is calculated for the following direct and indirect climate forcers: CO_2, CH_4, N_2O, O_3, SF_6, 29 halocarbon species, OH, VOC, CO, NO_x, stratospheric H_2O, sulfate aerosols, and carbonaceous aerosols (both direct and indirect effects). The changes in CH_4 and N_2O concentrations are given as a function of their atmospheric concentrations, the sum of anthropogenic and natural emissions, and their lifetime. ACC2 accounts for nonlinear feedbacks such as the saturation of ocean CO_2 uptake under rising CO_2 concentration, CO_2 fertilization of the land biosphere, and increasing heterotrophic respiration of the land biosphere with rising temperatures. Furthermore, uncertain parameters in ACC2 are calibrated with a Bayesian approach[13,22]. The model is developed in the GAMS programming language and numerically solved using CONOPT3 and CONOPT4, two nonlinear optimization solvers included in the GAMS software package. When ACC2 is used as a simulator, the first three modules are used to calculate temperature changes based on prescribed emissions scenarios. On the other hand, when ACC2 is used as an optimizer, all four modules, including the economy module consisting of the marginal abatement cost curves[50] for global CO_2, CH_4, and N_2O emissions, are used to derive least-cost emission pathways for a given climate target. ACC2 has participated in model intercomparison projects[21,49] and has been subject to comparison with other models in other studies[66]. This model has been applied to analyze pathways to achieve the targets of the Paris Agreement[9,22,67] including GHG removal options[68]. The performance of ACC2 configured for this paper with three EMSs was benchmarked against other simple climate models under commonly used scenarios RCP2.6 and RCP4.5 in the emission-driven mode[49] (Figs. S10 and S11).

Carbon cycle parameters in ACC2

As in many simple climate and carbon cycle models, a steady state is assumed for the carbon cycle in the preindustrial period[69]. In 1750, the preindustrial start year of ACC2, the Net Primary Production (NPP) was assumed to be constant and in balance with the heterotrophic respiration. The perturbation of the NPP and the resulting changes in heterotrophic respiration are described by the four-reservoir land box model. A change in atmospheric CO_2 concentration logarithmically influences the NPP (i.e., CO_2 fertilization), the strength of which is scaled with the BETA factor. On the other hand, the heterotrophic respiration is exponentially dependent on the temperature as parameterized through a Q10 factor, at the rate of which the heterotrophic respiration increases with a temperature increase of 10 °C.

The governing equation for each of the four land reservoirs is:

$$\dot{c}_{ter,l}(t) = A_{ter,l}\tau_{ter,l}\left(\bar{f}^{pre}_{NPP} + \delta f_{NPP}(t)\right) - \frac{1}{\tau_{ter,l}}\left(\bar{c}^{pre}_{ter,l} + c_{ter,l}(t)\right)q(t) \text{with } l = [1\text{-}4] \quad (3)$$

Here, the first term on the right-hand side of Eq. (3) represents added carbon to the reservoir *l*: the increase in NPP of year *t* ($\delta f_{NPP}(t)$) combined with the preindustrial constant NPP ($\bar{f}^{pre}_{NPP}$). $A_{ter,l}$ and $\tau_{ter,l}$ represents the coefficients and the overturning time constants of the IRF describing the temporal evolution of biomass for each reservoir. The second term represents released carbon from the reservoir *l*: the release of carbon from both

preindustrial ($\bar{c}^{pre}_{ter,l}$) and fertilized storage ($c_{ter,l}(t)$), which can be enhanced under warming through $q(t)$, the Q10 factor, accounting for climate-carbon cycle feedbacks.

Furthermore, the BETA (β_{NPP}) and Q10 factors used to parameterize the CO_2 fertilization effect on photosynthesis and temperature control on heterotrophic respiration, respectively, are expressed in the two following equations:

$$\delta f_{NPP}(t) = \bar{f}^{pre}_{NPP}\beta_{NPP}\ln\left(\frac{pCO_2(t)}{pCO_2^{pre}}\right) \quad (4)$$

$$q(t) = Q_{10}\frac{\delta T_{land-air}(t)}{10} \quad (5)$$

Note that the BETA factor is a commonly used parameter representing the CO_2 fertilization effect (more technically, a scaling parameter expressing the sensitivity of the change in NPP to the logarithmic change in atmospheric CO_2 concentrations) but importantly differs from another commonly used parameter β also representing a quantity including the CO_2 fertilization effect (a scaling parameter expressing the sensitivity of the carbon storage to the change in atmospheric CO_2 concentrations, expressed in GtC ppm^{-1})[62,70–72].

Emulating ACC2 to CMIP6 ESMs

We emulated ACC2 to five state-of-the-art ESMs (CanESM5, CNRM-ESM2-1, IPSL-CM6A-LR, MIROC-ES2L, and UKESM1-0-LL, see Table S2 for an overview of the ESMs) developed under the Coupled Model Intercomparison Project 6, CMIP6[73]. The emulation was performed using SSP5-3.4-OS, a high-temperature overshoot scenario combining the high emission SSP5-8.5 scenario until 2040 with strong mitigation thereafter[74]. We used the data from the fully-coupled (COU) configuration of ESMs. Our emulation method focuses only on three key parameters: namely, the equilibrium climate sensitivity (ECS), BETA, and Q10. Overall, three configurations of ACC2 emulating IPSL-CM6A-LR, CNRM-ESM2-1, and MIROC-ES2L have been used for the analysis because relatively large number of scenarios were obtained from these three configurations for the range of temperature targets and overshoot profiles considered in this study.

We first calibrated the ACC2 temperature response with that of each ESM. By tuning the ECS parameter in ACC2 (Table S3), we determined, for each ESM, the value of ECS which yielded the closest projection to each ESM (Fig. S13 and Table S4).

Then, we tuned BETA and Q10 values to emulate NBP (Table 2). We considered NBP to capture carbon concentration and carbon-climate feedback effects. We adjusted NBP estimates of ACC2 to correct for a lack of representation of land-use change (LUC) processes in ACC2. That is, LUC emissions data from the Global Carbon Budget[75] from 1850 to 2014 and integrated assessment models (IAM) output from 2015 to 2100 for the SSP5-3.4-OS[76,77] were used to make the ACC2 output comparable with ESMs. We identified the best combination of BETA and Q10 values for each ESM, for which the RMSE of the NBP estimates from ACC2 relative to the NBP from the ESM is minimized.

The results of the emulation process are shown in Table S4 and Figs. S14–S17. Our emulation for ACC2 gives similar or systematically lower ECS values compared to those reported elsewhere[78], with an average difference of 0.64 °C.

In Fig. S14, NBP from ACC2 with the best combination of BETA and Q10 values for each ESM is compared with NBP from the respective ESM. Apart from the inter-annual variability, the emulation shows overall a good performance for both the ramp-up and ramp-down phases. We further evaluated the emulation of IPSL-CM6A-LR with ACC2 by using the optimal combination of ECS, BETA, and Q10 parameters to simulate seven additional scenarios. Figures S15–S17 show the land carbon uptake, ocean carbon uptake, and temperature evolution from the emulated ACC2 and IPSL-CM6A-LR. The temperature change was reproduced very well overall for all the SSP scenarios considered. Some over-estimation of ocean carbon uptake, on the other hand, occurred in ACC2 when the ocean carbon uptake declined. This inconsistency may be related to a faster mixing of carbon from the surface to the deep ocean in simple climate models[66]. Land carbon uptake showed a significant misfit in the cases of medium to high forcing scenarios (SSP2-4.5, SSP4-6.0, and SSP3-7.0, and SSP5-8.5), which gives >3 °C warming at the end of this century. The largest warming level considered in our analysis using the ranges of overshoot scenarios (Figs. 2, 3) is approximately 3 °C (or 1 °C overshoot of the 2 °C target level). Thus, the misfit found here does not pose a problem for our application, given the range of our model application.

Data availability

The data used for replicating the analysis and the figures presented in this work can be found in the following GitHub repository: https://github.com/Matteo-Mastro/GWP_overshoot.git.

Code availability

The codes used for replicating the analysis and the figures presented in this work can be found in the following GitHub repository: https://github.com/Matteo-Mastro/GWP_overshoot.git.

Received: 26 July 2023; Accepted: 17 February 2025;
Published online: 12 March 2025

References

1. Myhre, G. et al. Anthropogenic and Natural Radiative Forcing. in *Climate Change 2013: The Physical Science Basis. Contribution of Working Group I to the Fifth Assessment Report of the Intergovernmental Panel on Climate Change* (Cambridge University Press, Cambridge, United Kingdom and New York, NY, USA, 2013).
2. Tanaka, K., Peters, G. P. & Fuglestvedt, J. S. Policy update: multicomponent climate policy: why do emission metrics matter? *Carbon Manag.* **1**, 191–197 (2010).
3. Lashof, D. A. & Ahuja, D. R. Relative contributions of greenhouse gas emissions to global warming. *Nature* **344**, 529–531 (1990).
4. UNFCCC. Common metrics | UNFCCC. https://unfccc.int/process-and-meetings/transparency-and-reporting/methods-for-climate-change-transparency/common-metrics (2023).
5. Shine, K. P., Berntsen, T. K., Fuglestvedt, J. S., Skeie, R. B. & Stuber, N. Comparing the climate effect of emissions of short- and long-lived climate agents. *Philos. Trans. R. Soc. A Math. Phys. Eng. Sci.* **365**, 1903–1914 (2007).
6. Manne, A. S. & Richels, R. G. An alternative approach to establishing trade-offs among greenhouse gases. *Nature* **410**, 675–677 (2001).
7. O'Neill, B. C. Economics, natural science, and the costs of global warming potentials. *Clim. Change* **58**, 251–260 (2003).
8. Tol, R. S. J., Berntsen, T. K., O'Neill, B. C., Fuglestvedt, J. S. & Shine, K. P. A unifying framework for metrics for aggregating the climate effect of different emissions. *Environ. Res. Lett.* **7**, 044006 (2012).
9. Tanaka, K., Boucher, O., Ciais, P., Johansson, D. J. A. & Morfeldt, J. Cost-effective implementation of the Paris Agreement using flexible greenhouse gas metrics. *Sci. Adv.* **7** (2021).
10. UNFCCC. Report of the Conference of the Parties serving as the meeting of the Parties to the Paris Agreement on the third part of its first session, held in Katowice from 3 to 14 December 2018. Addendum 2. (2018).
11. Allen, M. R. et al. Indicate separate contributions of long-lived and short-lived greenhouse gases in emission targets. *NPJ Clim. Atmos. Sci.* **5**, 1–4 (2022). *2022 5:1*.
12. Wigley, T. M. L. The Kyoto Protocol: CO_2 CH_4 and climate implications. *Geophys. Res. Lett.* **25**, 2285–2288 (1998).
13. Tanaka, K. et al. Evaluating global warming potentials with historical temperature. *Clim. Change* **96**, 443–466 (2009).
14. Tanaka, K., Johansson, D. J. A., O'Neill, B. C. & Fuglestvedt, J. S. Emission metrics under the 2 °C climate stabilization target. *Clim. Change* **117**, 933–941 (2013).

15. Allen, M. R. et al. A solution to the misrepresentations of CO_2-equivalent emissions of short-lived climate pollutants under ambitious mitigation. *NPJ Clim. Atmos. Sci.* **1**, 1–8 (2018). *2018 1:1*.
16. Cain, M. et al. Improved calculation of warming-equivalent emissions for short-lived climate pollutants. *NPJ Clim. Atmos. Sci.* **2**, 1–7 (2019). *2019 2:1*.
17. Fuglestvedt, J. S. et al. Metrics of climate change: assessing radiative forcing and emission indices. *Clim. Change* **58**, 267–331 (2003).
18. Pierrehumbert, R. T. Short-lived climate pollution. *Annu. Rev. Earth Planet. Sci.* **42**, 341–379 (2014).
19. Archer, D. et al. Atmospheric lifetime of fossil fuel carbon dioxide. *Annu. Rev. Earth Planet. Sci.* **37**, 117–134 (2009).
20. Eby, M. et al. Lifetime of anthropogenic climate change: millennial time scales of potential CO_2 and surface temperature perturbations. *J. Clim.* **22**, 2501–2511 (2009).
21. Joos, F. et al. CO_2 and climate impulse response functions for metric computation atmospheric chemistry and physics discussions carbon dioxide and climate impulse response functions for the computation of greenhouse gas metrics: a multi-model analysis. *Atmos. Chem. Phys. Discuss* **12**, 2793–2825 (2013).
22. Tanaka, K. & O'Neill, B. C. The Paris Agreement zero-emissions goal is not always consistent with the 1.5 °C and 2 °C temperature targets. *Nat. Clim. Change* **8**, 319–324 (2018). *2018 8:4*.
23. Allen, M. R. et al. Warming caused by cumulative carbon emissions towards the trillionth tonne. *Nature* **458**, 1163–1166 (2009).
24. Matthews, H. D., Gillett, N. P., Stott, P. A. & Zickfeld, K. The proportionality of global warming to cumulative carbon emissions. *Nature* **459**, 829–832 (2009).
25. Rogelj, J., Forster, P. M., Kriegler, E., Smith, C. J. & Séférian, R. Estimating and tracking the remaining carbon budget for stringent climate targets. *Nature* **571**, 335–342 (2019).
26. Damon Matthews, H. et al. An integrated approach to quantifying uncertainties in the remaining carbon budget. *Commun. Earth Environ.* **2**, 7 (2021).
27. Jenkins, S. et al. Quantifying non-CO_2 contributions to remaining carbon budgets. *NPJ Clim. Atmos. Sci.* **4**, 47 (2021).
28. Lynch, J., Cain, M., Pierrehumbert, R. & Allen, M. Demonstrating GWP*: a means of reporting warming-equivalent emissions that captures the contrasting impacts of short- and long-lived climate pollutants. *Environ. Res. Lett.* **15**, 044023 (2020).
29. Mengis, N. & Matthews, H. D. Non-CO_2 forcing changes will likely decrease the remaining carbon budget for 1.5 °C. *NPJ Clim. Atmos. Sci.* **3**, 1–7 (2020).
30. Smith, S. M. et al. Equivalence of greenhouse-gas emissions for peak temperature limits. *Nat. Clim. Change* **2**, 535–538 (2012).
31. Allen, M. R. et al. New use of global warming potentials to compare cumulative and short-lived climate pollutants. *Nat. Clim. Change* **6**, 773–776 (2016).
32. Smith, M. A., Cain, M. & Allen, M. R. Further improvement of warming-equivalent emissions calculation. *NPJ Clim. Atmos. Sci.* **4**, 1–3 (2021).
33. Forster, P. et al. The Earth's energy budget, climate feedbacks, and climate sensitivity. in *Climate Change 2021: The Physical Science Basis. Contribution of Working Group I to the Sixth Assessment Report of the Intergovernmental Panel on Climate Change* 923–1054 (Cambridge University Press, Cambridge, United Kingdom and New York, NY, USA, 2021).
34. Dhakal, S. et al. Emissions Trends and Drivers. in *Climate Change 2022: Mitigation of Climate Change* (IPCC: Intergovernmental Panel on Climate Change, 2022).
35. Canadell, J. G. et al. Global carbon and other biogeochemical cycles and feedbacks. in *Climate Change 2021: The Physical Science Basis. Contribution of Working Group I to the Sixth Assessment Report of the Intergovernmental Panel on Climate Change* 673–816 (Cambridge University Press, Cambridge, United Kingdom and New York, NY, USA, 2021).
36. Tokarska, K. B. et al. Uncertainty in carbon budget estimates due to internal climate variability. *Environ. Res. Lett.* **15**, 104064 (2020).
37. Rogelj, J. et al. Paris Agreement climate proposals need a boost to keep warming well below 2 °C. *Nature* **534**, 631–639 (2016).
38. Jenkins, S., Millar, R. J., Leach, N. & Allen, M. R. Framing climate goals in terms of cumulative CO_2-forcing-equivalent emissions. *Geophys. Res. Lett.* **45**, 2795–2804 (2018).
39. Rogelj, J. et al. Mitigation pathways compatible with 1.5°C in the context of sustainable development. in *Global warming of 1.5 Global Warming of 1.5°C. An IPCC Special Report on the impacts of global warming of 1.5°C above pre-industrial levels and related global greenhouse gas emission pathways, in the context of strengthening the global response to the threat of climate change, sustainable development, and efforts to eradicate poverty* 93–174 (Cambridge University Press, Cambridge, United Kingdom and New York, NY, USA, 2018).
40. Johansson, D. J. A. The question of overshoot. *Nat. Clim. Chang.* **11**, 1021–1022 (2021).
41. Riahi, K. et al. Cost and attainability of meeting stringent climate targets without overshoot. *Nat. Clim. Chang.* **11**, 1063–1069 (2021).
42. Bossy, T., Gasser, T., Tanaka, K. & Ciais, P. On the chances of staying below the 1.5°C warming target. *Cell Rep. Sustain.y* **0**, 100127 (2024).
43. Schmidt, G. Climate models can't explain 2023's huge heat anomaly —we could be in uncharted territory. *Nature* **627**, 467–467 (2024).
44. Cherubini, F. et al. Bridging the gap between impact assessment methods and climate science. *Environ. Sci. Policy* **64**, 129–140 (2016).
45. Tanaka, K., Cavalett, O., Collins, W. J. & Cherubini, F. Asserting the climate benefits of the coal-to-gas shift across temporal and spatial scales. *Nat. Clim. Change* **9**, 389–396 (2019).
46. Levasseur, A. et al. Enhancing life cycle impact assessment from climate science: Review of recent findings and recommendations for application to LCA. *Ecol. Indic.* **71**, 163–174 (2016). (2016).
47. Allen, M. et al. Ensuring that offsets and other internationally transferred mitigation outcomes contribute effectively to limiting global warming. *Environ. Res. Lett.* **16**, 074009–074009 (2021).
48. Tanaka, K. et al. Aggregated Carbon cycle, atmospheric chemistry and climate model (ACC2): description of forward and inverse mode. (2007).
49. Nicholls, Z. et al. Reduced complexity model intercomparison project phase 1: introduction and evaluation of global-mean temperature response. *Geosci. Model Dev.* **13**, 5175–5190 (2020).
50. Xiong, W., Tanaka, K., Ciais, P., Johansson, D. J. A. & Lehtveer, M. emIAM v1.0: an emulator for Integrated Assessment Models using marginal abatement cost curves. *Geosci. Model Dev.* (2023) https://doi.org/10.5194/egusphere-2022-1508.
51. Rogelj, J. et al. A new scenario logic for the Paris Agreement long-term temperature goal. *Nature* **573**, 357–363 (2019).
52. Emmerling, J. et al. The role of the discount rate for emission pathways and negative emissions. *Environ. Res. Lett.* **14**, 104008 (2019).
53. Rogelj, J. et al. Scenarios towards limiting global mean temperature increase below 1.5 °C. *Nat. Clim. Change* **8**, 325–332 (2018).
54. Zickfeld, K., MacDougall, A. H. & Matthews, H. D. On the proportionality between global temperature change and cumulative CO_2 emissions during periods of net negative CO_2 emissions. *Environ. Res. Lett.* **11**, 055006–055006 (2016).
55. Tokarska, K. B., Zickfeld, K. & Rogelj, J. Path independence of carbon budgets when meeting a stringent global mean temperature target after an overshoot. *Earth's. Future* **7**, 1283–1295 (2019).
56. Keller, D. P. et al. The carbon dioxide removal model intercomparison project (CDRMIP): rationale and experimental protocol for CMIP6. *Geosci. Model Dev.* **11**, 1133–1160 (2018).
57. Jones, C. D. et al. The zero emissions commitment model intercomparison project (ZECMIP) contribution to C4MIP: quantifying committed climate changes following zero carbon emissions. *Geosci. Model Dev.* **12**, 4375–4385 (2019).

58. MacDougall, A. H. et al. Is there warming in the pipeline? A multi-model analysis of the zero emissions commitment from CO_2. *Biogeosciences* **17**, 2987–3016 (2020).
59. Canadell, J. G. et al. Global carbon and other biogeochemical cycles and feedbacks. (2022).
60. Zickfeld, K., Azevedo, D., Mathesius, S. & Damon Matthews, H. Asymmetry in the climate–carbon cycle response to positive and negative CO2 emissions. *Nat. Clim. Change* **11**, 613–617 (2021).
61. Tachiiri, K., Hajima, T. & Kawamiya, M. Increase of the transient climate response to cumulative carbon emissions with decreasing CO_2 concentration scenarios. *Environ. Res. Lett.* **14**, 124067 (2019).
62. Melnikova, I. et al. Carbon cycle response to temperature overshoot beyond 2°C: an analysis of CMIP6 models. *Earth's Future* **9**, e2020EF001967 (2021).
63. Smith, C. J. et al. FAIR v1.3: a simple emissions-based impulse response and carbon cycle model. *Geosci. Model Dev.* **11**, 2273–2297 (2018).
64. Millar, R. J., Nicholls, Z. R., Friedlingstein, P. & Allen, M. R. A modified impulse-response representation of the global near-surface air temperature and atmospheric concentration response to carbon dioxide emissions. *Atmos. Chem. Phys.* **17**, 7213–7228 (2017).
65. Lynch, J., Cain, M., Frame, D. & Pierrehumbert, R. Agriculture's contribution to climate change and role in mitigation is distinct from predominantly fossil CO_2-emitting sectors. *Front. Sustain. Food Syst.* **4**, 300–300 (2021).
66. Melnikova, I., Ciais, P., Boucher, O. & Tanaka, K. Assessing carbon cycle projections from complex and simple models under SSP scenarios. *Clim. Change* **176**, 168 (2023).
67. Xiong, W., Tanaka, K., Ciais, P. & Yan, L. Evaluating China's role in achieving the 1.5 °C Target of the Paris Agreement. *Energies* **15**, 6002 (2022).
68. Gaucher, Y., Tanaka, K., Johansson, D. J. A., Boucher, O. & Ciais, P. Potential and costs required for methane removal to compete with BECCS as a mitigation option.
69. Mackenzie, F. T. & Lerman, A. *Carbon in the Geobiosphere:-Earth's Outer Shell*. 25 (Springer Science & Business Media, 2006).
70. Friedlingstein, P. et al. Climate–carbon cycle feedback analysis: results from the C4MIP model intercomparison. *J. Clim.* **19**, 3337–3353 (2006).
71. Gregory, J. M., Jones, C. D., Cadule, P. & Friedlingstein, P. Quantifying carbon cycle feedbacks. *J. Clim.* **22**, 5232–5250 (2009).
72. Jones, C. D. et al. C4MIP-the coupled climate-carbon cycle model intercomparison project: experimental protocol for CMIP6. *Geosci. Model Dev.* **9**, 2853–2880 (2016).
73. Eyring, V. et al. Overview of the coupled model intercomparison project phase 6 (CMIP6) experimental design and organization. *Geosci. Model Dev.* **9**, 1937–1958 (2016).
74. O'Neill, B. C. et al. The scenario model intercomparison project (ScenarioMIP) for CMIP6. *Geosci. Model Dev.* **9**, 3461–3482 (2016).
75. Friedlingstein, P. et al. Global carbon budget 2021. *Earth Syst. Sci. Data* **14**, 1917–2005 (2021).
76. Ackerman, F., DeCanio, S. J., Howarth, R. B. & Sheeran, K. Limitations of integrated assessment models of climate change. *Clim. change* **95**, 297–315 (2009).
77. Van Vuuren, D. P. et al. Energy, land-use and greenhouse gas emissions trajectories under a green growth paradigm. *Glob. Environ. Change* **42**, 237–250 (2017).
78. Zelinka, M. D. et al. Causes of higher climate sensitivity in CMIP6 models. *Geophys. Res. Lett.* **47**, e2019GL085782 (2020).

Acknowledgements

M.M. acknowledges financial support from the Italian Ministry of the University and Research, as well as the European Union for the Erasmus+ Traineeship scholarship. This research was conducted as part of the Achieving the Paris Agreement Temperature Targets after Overshoot (PRATO) Project under the Make Our Planet Great Again (MOPGA) Program and funded by the National Research Agency in France under the Programme d'Investissements d'Avenir, grant number. I.M. was supported by the Program for the Advanced Studies of Climate Change Projection (SENTAN, grant number JPMXD0722681344) from the Ministry of Education, Culture, Sports, Science and Technology (MEXT), Japan. We also acknowledge the European Union's Horizon Europe research and innovation programme under Grant Agreements N° 101056939 (RESCUE—Response of the Earth System to overshoot, Climate neUtrality, and negative Emissions) and N° 101081193 (OptimESM—Optimal High Resolution Earth System Models for Exploring Future Climate Changes).

Author contributions

Conceptualization of the research, K.T.; simulations using IRF, FaIR and ACC2, M.M. and K.T.; analysis of simulations results, M.M, K.T.; writing—original draft preparation, M.M. and K.T.; Tuning of ACC2 with ESMs, M.M., I.M., and K.T.; writing—revision and editing, M.M., K.T., I.M., P.C.; All authors have read and agreed to the submitted version of the manuscript.

Competing interests

The authors declare no competing interest

Additional information

Supplementary information The online version contains supplementary material available at https://doi.org/10.1038/s41612-025-00980-7.

Correspondence and requests for materials should be addressed to Matteo Mastropierro or Katsumasa Tanaka.